

## 4. Shear strength of discontinuities

### Introduction

All rock masses contain discontinuities such as bedding planes, joints, shear zones and faults. At shallow depth, where stresses are low, failure of the intact rock material is minimal and the behaviour of the rock mass is controlled by sliding on the discontinuities. In order to analyse the stability of this system of individual rock blocks, it is necessary to understand the factors that control the shear strength of the discontinuities which separate the blocks. These questions are addressed in the discussion that follows.

### Shear strength of planar surfaces

Suppose that a number of samples of a rock are obtained for shear testing. Each sample contains a through-going plane that is cemented; in other words, a tensile force would have to be applied to the two halves of the specimen in order to separate them. The plane is absolutely planar, having no surface irregularities or undulations. As illustrated in Figure 1, the specimen is subjected to a stress  $\sigma_n$  normal to the plane, and the shear stress  $\tau$ , required to cause a displacement  $\delta$ , is measured.

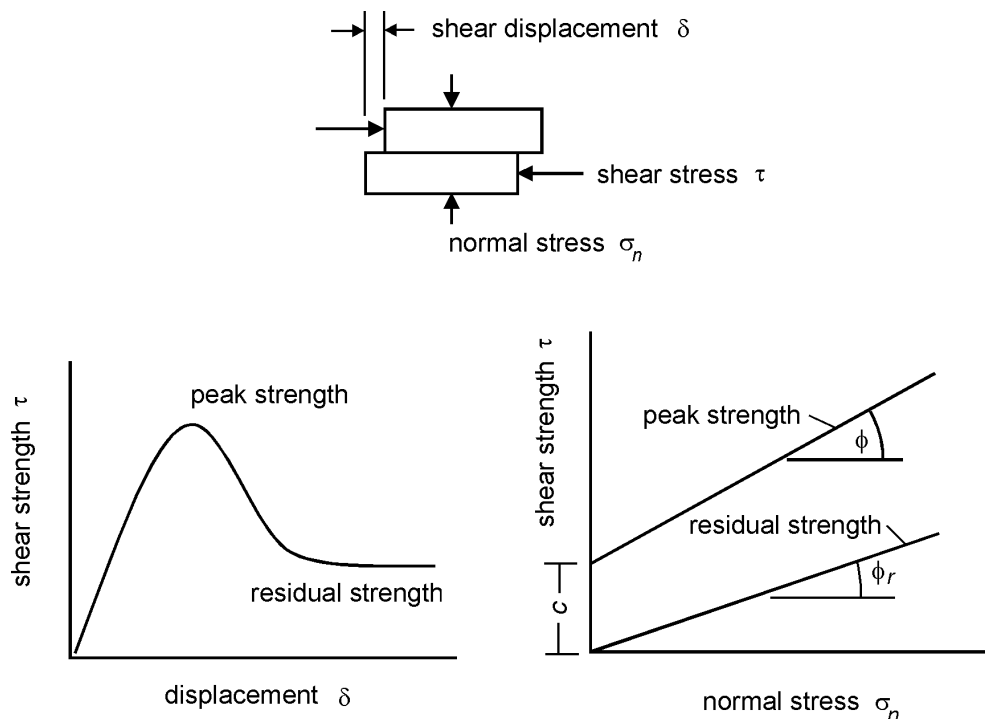


Figure 1: Shear testing of discontinuities.

The shear stress will increase rapidly until the peak strength is reached. This corresponds to the sum of the strength of the cementing material bonding the two halves of the bedding plane together and the frictional resistance of the matching surfaces. As the displacement continues, the shear stress will fall to a residual value that will then remain constant, even for large shear displacements.

Plotting the peak and residual shear strengths for different normal stresses results in the two lines illustrated in Figure 1. For planar discontinuity surfaces the experimental points will generally fall along straight lines. The peak strength line has a slope of  $\phi$  degrees and an intercept of  $c$  on the shear strength axis. The residual strength line has a slope of  $\phi_r$ .

The relationship between the peak shear strength  $\tau_p$  and the normal stress  $\sigma_n$  can be represented by the Mohr-Coulomb equation:

$$\tau_p = c + \sigma_n \tan \phi \quad (1)$$

where  $c$  is the cohesive strength of the cemented surface and  $\phi$  is the angle of friction.

In the case of the residual strength, the cohesion  $c$  has dropped to zero and the relationship between  $\phi_r$  and  $\sigma_n$  can be represented by:

$$\tau_r = \sigma_n \tan \phi_r \quad (2)$$

where  $\phi_r$  is the residual angle of friction.

This example has been discussed in order to illustrate the physical meaning of the term cohesion, a soil mechanics term, which has been adopted by the rock mechanics community. In shear tests on soils, the stress levels are generally an order of magnitude lower than those involved in rock testing and the cohesive strength of a soil is a result of the adhesion of the soil particles. In rock mechanics, true cohesion occurs when cemented surfaces are sheared. However, in many practical applications, the term cohesion is used for convenience and it refers to a mathematical quantity related to surface roughness, as discussed in a later section. Cohesion is defined by the intercept on the shear strength axis  $\tau$  at zero normal stress.

The basic friction angle  $\phi_b$  is a quantity that is fundamental to the understanding of the shear strength of discontinuity surfaces. This is approximately equal to the residual friction angle  $\phi_r$  and it is generally measured by testing sawn or ground rock surfaces. These tests, which can be carried out on surfaces as small as 50 mm  $\times$  50 mm, will produce a straight-line plot.

A typical shear testing machine, which can be used to determine the basic friction angle  $\phi_b$  is illustrated in Figures 2 and 3. This is a very simple machine and the use of a mechanical lever arm ensures that the normal load on the specimen remains constant throughout the test. This is an important practical consideration since it is difficult to maintain a constant normal load in hydraulically or pneumatically controlled systems. Note that it is important in setting up the specimen that care has to be taken to ensure that the shear surface is aligned accurately in order to avoid the need for an additional angle correction.

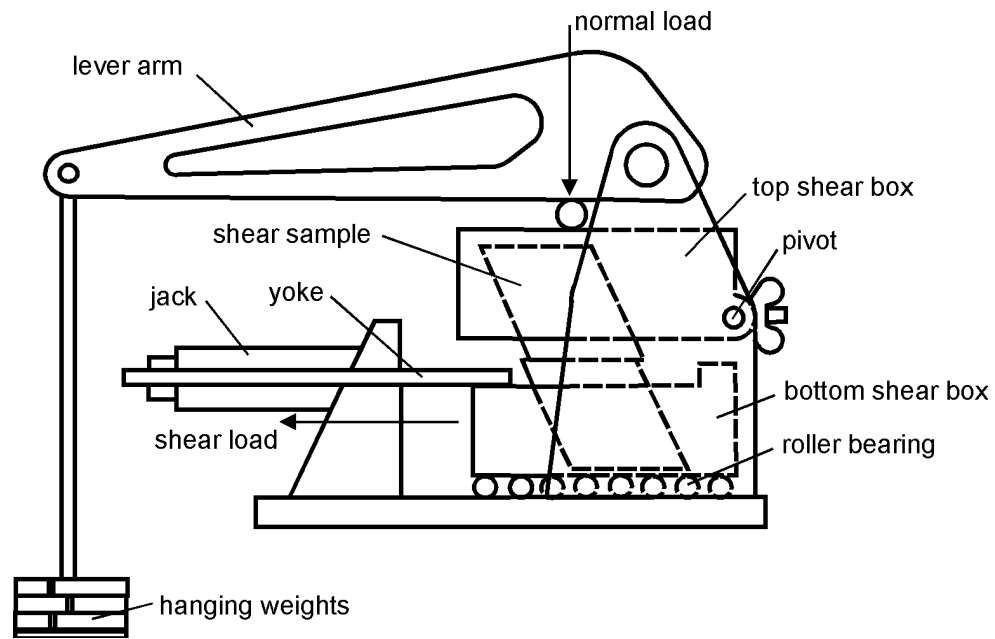


Figure 2: Diagrammatic section through shear machine used by Hencher and Richards (1982).

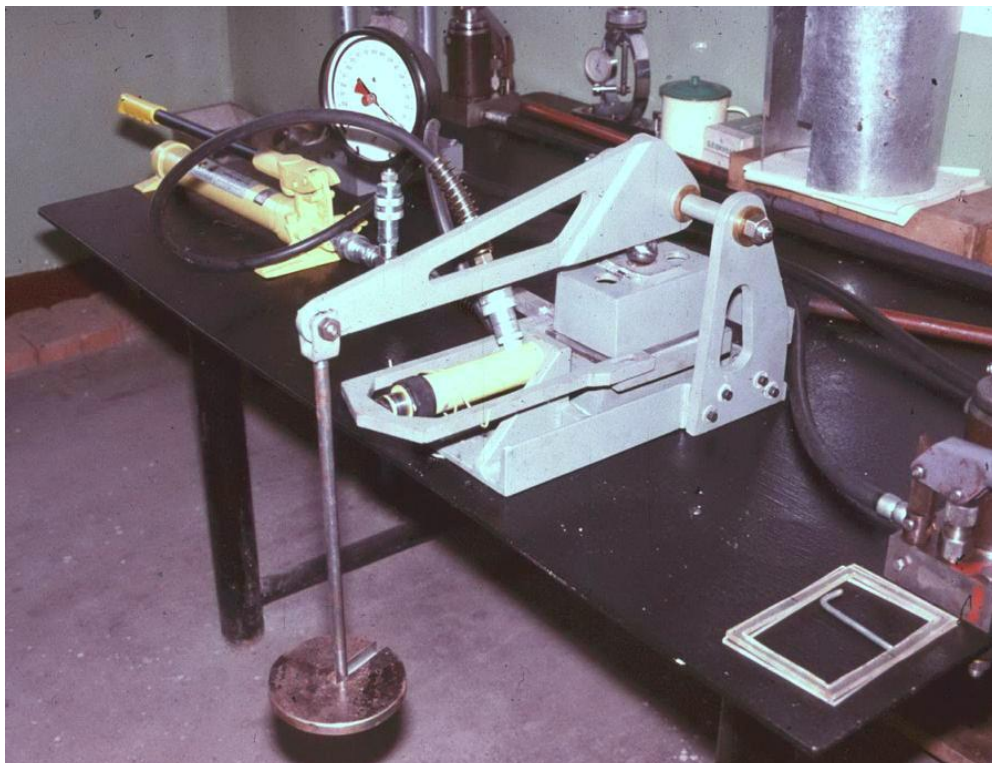


Figure 3: Shear machine of the type used by Hencher and Richards (1982) for measurement of the shear strength of sheet joints in Hong Kong granite.

Most shear strength tests today are carried out by determining the basic friction angle, as described above, and then making corrections for surface roughness as discussed in the following sections of this chapter. In the past there was more emphasis on testing full scale discontinuity surfaces, either in the laboratory or in the field. There are a significant number of papers in the literature of the 1960s and 1970s describing large and elaborate in situ shear tests, many of which were carried out to determine the shear strength of weak layers in dam foundations. However, the high cost of these tests together with the difficulty of interpreting the results has resulted in a decline in the use of these large-scale tests which are seldom seen today.

The author's opinion is that it makes both economical and practical sense to carry out a number of small-scale laboratory shear tests, using equipment such as that illustrated in Figures 2 and 3, to determine the basic friction angle. The roughness component is added to this basic friction angle to give the effective friction angle, which is site specific and scale dependent and is best obtained by visual estimates in the field. Practical techniques for making these roughness angle estimates are described on the following pages.

### Shear strength of rough surfaces

A natural discontinuity surface in hard rock is never as smooth as a sawn or ground surface of the type used for determining the basic friction angle. The undulations and asperities on a natural joint surface have a significant influence on its shear behaviour. Generally, this surface roughness increases the shear strength of the surface, and this strength increase is extremely important in terms of the stability of excavations in rock.

Patton (1966) demonstrated this influence by means of an experiment in which he carried out shear tests on 'saw-tooth' specimens such as the one illustrated in Figure 4. Shear displacement in these specimens occurs as a result of the surfaces moving up the inclined faces, causing dilation (an increase in volume) of the specimen.

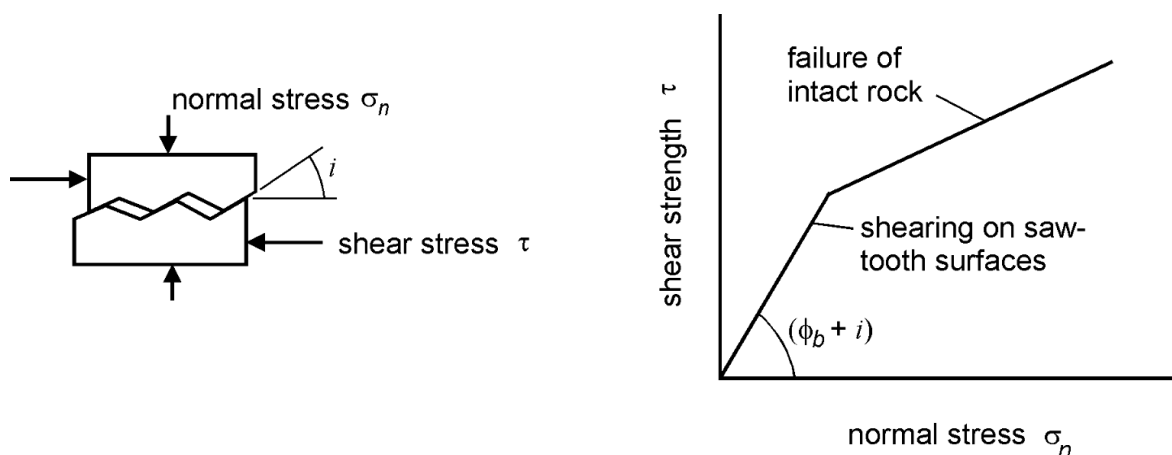


Figure 4: Patton's experiment on the shear strength of saw-tooth specimens.

The shear strength of Patton's saw-tooth specimens can be represented by:

$$\tau = \sigma_n \tan(\phi_b + i) \quad (3)$$

where  $\phi_b$  is the basic friction angle of the surface and  
 $i$  is the angle of the saw-tooth face.

Equation 3 is valid for low normal stresses where shear displacement is due to sliding along the inclined surfaces. At higher normal stresses the strength of the intact material will be exceeded and the teeth will break off, resulting in a shear strength behaviour which is related to failure of the intact rock material.

### **Barton's estimate of shear strength**

While Patton's approach has the merit of being very simple, it does not reflect the reality that changes in shear strength with increasing normal stress are gradual rather than abrupt. Barton (1973, 1976) studied the behaviour of natural rock joints and proposed that equation (3) could be re-written as:

$$\tau = \sigma_n \tan\left(\phi_b + JRC \log_{10}\left(\frac{JCS}{\sigma_n}\right)\right) \quad (4)$$

where  $JRC$  is the joint roughness coefficient and  
 $JCS$  is the joint wall compressive strength.

Barton developed his first non-linear strength criterion for rock joints (using the basic friction angle  $\phi_b$ ) from analysis of joint strength data reported in the literature. Barton and Choubey (1977), on the basis of their direct shear test results for 130 samples of variably weathered rock joints, revised equation 4 to the following equation:

$$\tau = \sigma_n \tan\left(\phi_r + JRC \log_{10}\left(\frac{JCS}{\sigma_n}\right)\right) \quad (5)$$

where  $\phi_r$  is the residual friction angle which Barton and Choubey suggest can be estimated from

$$\phi_r = (\phi_b - 20) + 20(r/R) \quad (6)$$

where  $r$  is the Schmidt rebound number for wet and weathered fracture surfaces and  $R$  is the Schmidt rebound number for dry, unweathered, sawn surfaces.

Equations 5 and 6 have become part of the Barton-Bandis criterion for rock joint strength and deformability (Barton and Bandis, 1990).

### Field estimates of *JRC*

The joint roughness coefficient *JRC* is a number that can be estimated by comparing the appearance of a discontinuity surface with standard profiles published by Barton and others. One of the most useful of these profile sets was published by Barton and Choubey (1977) and is reproduced in Figure 5.

The appearance of the discontinuity surface in the rock specimen is compared visually with the profiles shown in Figure 5 and the *JRC* value corresponding to the profile which most closely matches that of the discontinuity surface is chosen. In the case of small-scale laboratory specimens, the scale of the surface roughness will be approximately the same as that of the profiles illustrated. However, in the field, the length of the surface of interest may be several metres or even tens of metres and the *JRC* value must be estimated for the full-scale surface.

An alternative method for estimating *JRC* is presented in Figure 6.

### Field estimates of *JCS*

Suggested methods for estimating the joint wall compressive strength were published by the ISRM (1978). The use of the Schmidt rebound hammer for estimating joint wall compressive strength was proposed by Deere and Miller (1966), as illustrated in Figure 7.

### Influence of scale on *JRC* and *JCS*

On the basis of extensive testing of joints, joint replicas, and a review of literature, Barton and Bandis (1982) proposed the scale corrections for *JRC* defined by the following relationship:


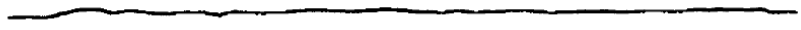

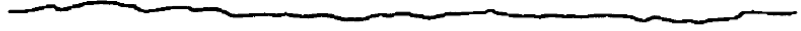
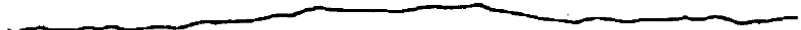






$$JRC_n = JRC_o \left( \frac{L_n}{L_o} \right)^{-0.02JRC_o} \quad (7)$$

where  $JRC_o$ , and  $L_o$  (length) refer to 100 mm laboratory scale samples and  $JRC_n$ , and  $L_n$  refer to in situ block sizes.

Because of the greater possibility of weaknesses in a large surface, it is likely that the average joint wall compressive strength (*JCS*) decreases with increasing scale. Barton and Bandis (1982) proposed the scale corrections for *JCS* defined by the following relationship:

$$JCS_n = JCS_o \left( \frac{L_n}{L_o} \right)^{-0.03JRC_o} \quad (8)$$

where  $JCS_o$  and  $L_o$  (length) refer to 100 mm laboratory scale samples and  $JCS_n$  and  $L_n$  refer to in situ block sizes.

	$JRC = 0 - 2$
	$JRC = 2 - 4$
	$JRC = 4 - 6$
	$JRC = 6 - 8$
	$JRC = 8 - 10$
	$JRC = 10 - 12$
	$JRC = 12 - 14$
	$JRC = 14 - 16$
	$JRC = 16 - 18$
	$JRC = 18 - 20$
 0 5 cm 10	

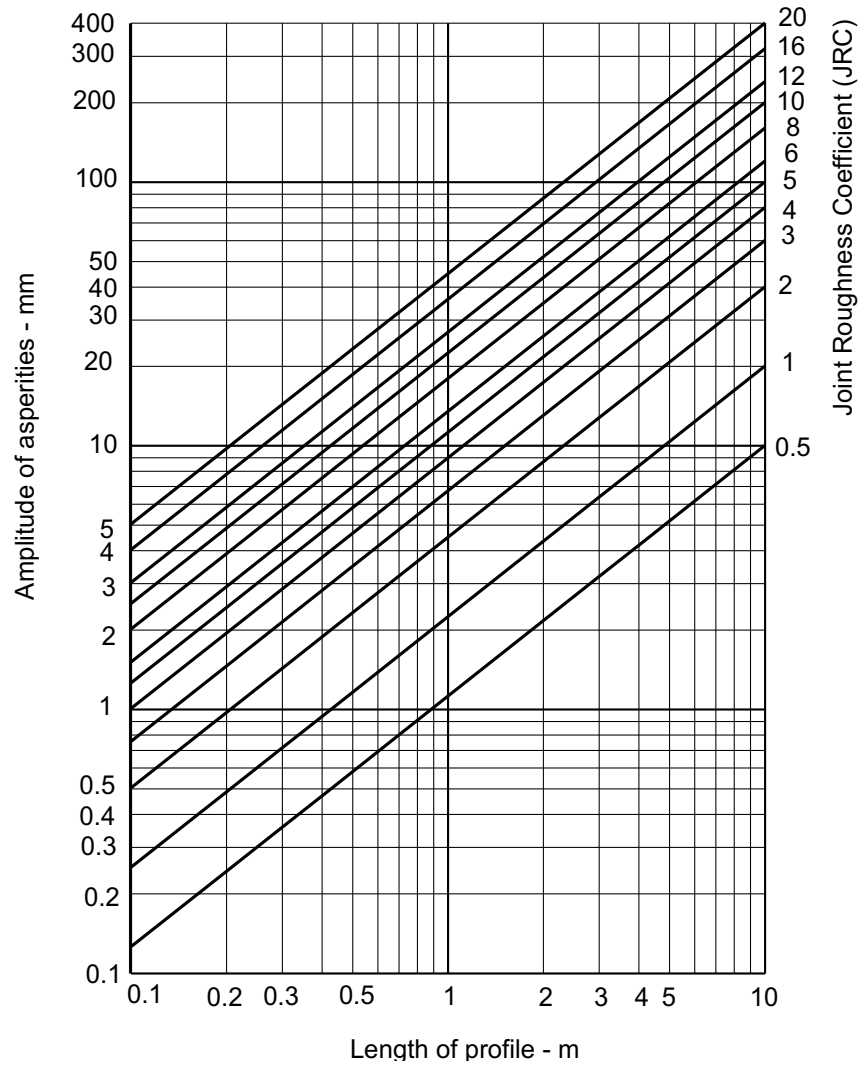
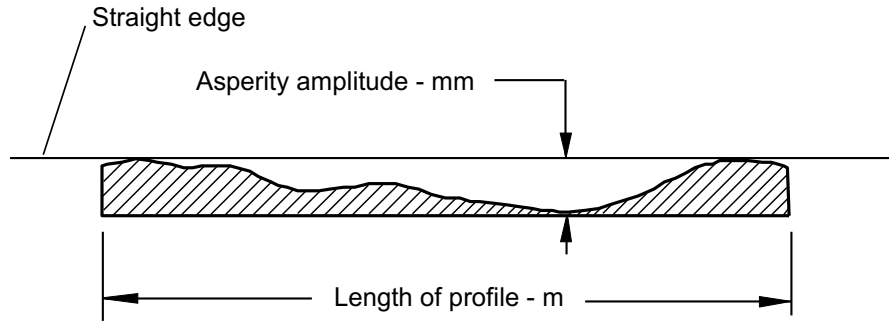


Figure 6: Alternative method for estimating  $JRC$  from measurements of surface roughness amplitude from a straight edge (Barton 1982).



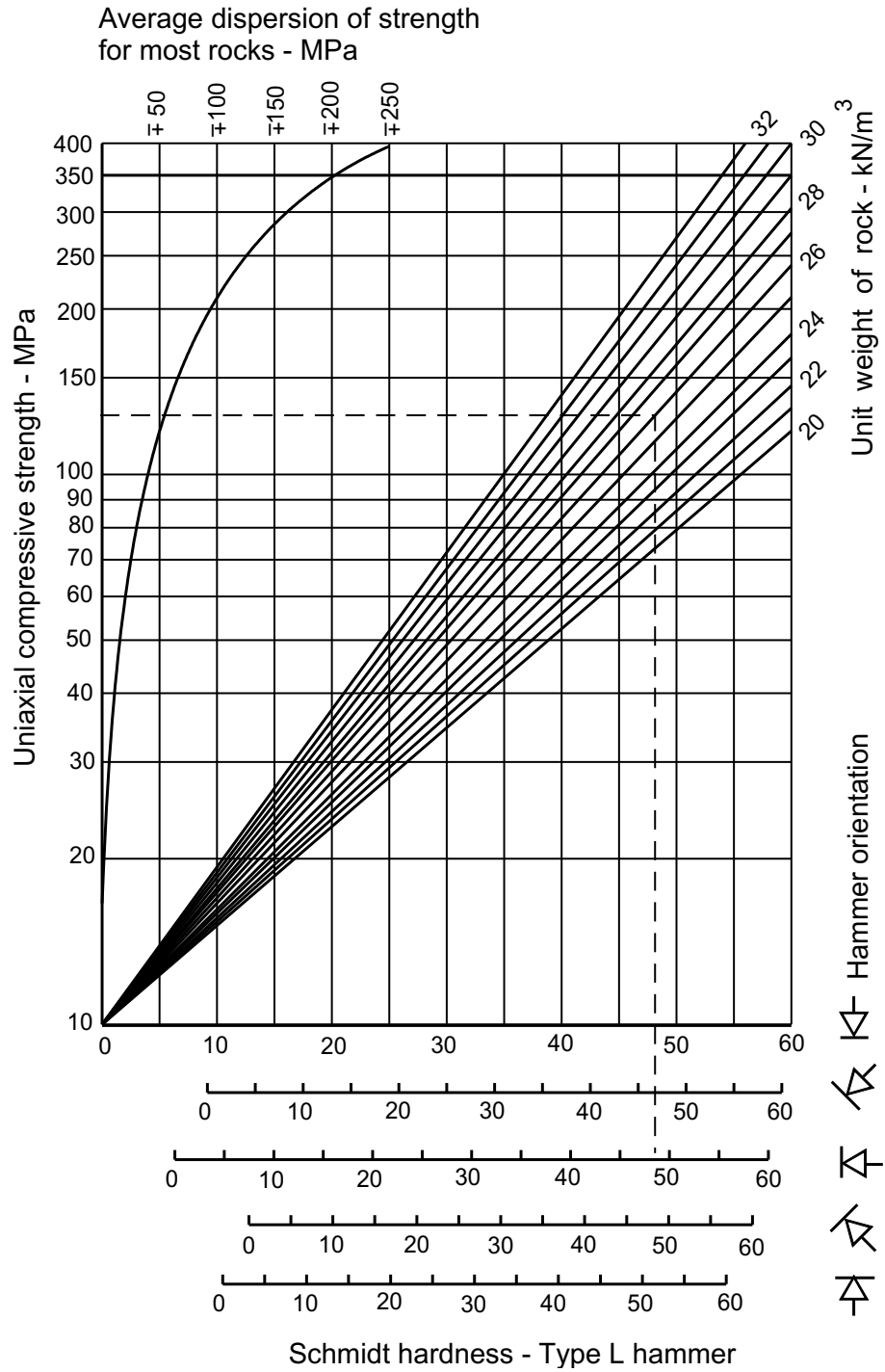


Figure 7: Estimate of joint wall compressive strength from Schmidt hardness.

## Shear strength of filled discontinuities

The discussion presented in the previous sections has dealt with the shear strength of discontinuities in which rock wall contact occurs over the entire length of the surface under consideration. This shear strength can be reduced drastically when part or all of the surface is not in intimate contact, but covered by soft filling material such as clay gouge. For planar surfaces, such as bedding planes in sedimentary rock, a thin clay coating will result in a significant shear strength reduction. For a rough or undulating joint, the filling thickness has to be greater than the amplitude of the undulations before the shear strength is reduced to that of the filling material.

A comprehensive review of the shear strength of filled discontinuities was prepared by Barton (1974) and a summary of the shear strengths of typical discontinuity fillings, based on Barton's review, is given in Table 1.

Where a significant thickness of clay or gouge fillings occurs in rock masses and where the shear strength of the filled discontinuities is likely to play an important role in the stability of the rock mass, it is strongly recommended that samples of the filling be sent to a soil mechanics laboratory for testing.

## Influence of water pressure

When water pressure is present in a rock mass, the surfaces of the discontinuities are forced apart and the normal stress  $\sigma_n$  is reduced. Under steady state conditions, where there is sufficient time for the water pressures in the rock mass to reach equilibrium, the reduced normal stress is defined by  $\sigma_n' = (\sigma_n - u)$ , where  $u$  is the water pressure. The reduced normal stress  $\sigma_n'$  is usually called the effective normal stress, and can be used in place of the normal stress term  $\sigma_n$  in all of the equations presented above.

## Instantaneous cohesion and friction

Due to the historical development of the subject of rock mechanics, many of the analyses, used to calculate factors of safety against sliding, are expressed in terms of the Mohr-Coulomb cohesion ( $c$ ) and friction angle ( $\phi$ ), defined in Equation 1. Since the 1970s, it has been recognised that the relationship between shear strength and normal stress is more accurately represented by a non-linear relationship such as that proposed by Barton and Bandis (1990). However, because this relationship is not expressed in terms of  $c$  and  $\phi$ , it is necessary to devise some means for estimating the equivalent cohesive strengths and angles of friction from relationships such as those proposed by Barton and Bandis.

Figure 8 gives definitions of the *instantaneous cohesion*  $c_i$  and the *instantaneous friction* angle  $\phi_i$  for a normal stress of  $\sigma_n$ . These quantities are given by the intercept and the inclination, respectively, of the tangent to the non-linear relationship between shear strength and normal stress. These quantities may be used for stability analyses in which the Mohr-Coulomb failure criterion (Equation 1) is applied, provided that the normal stress  $\sigma_n$  is reasonably close to the value used to define the tangent point.

Table 1: Shear strength of filled discontinuities and filling materials (After Barton 1974)

Rock	Description	Peak $c'$ (MPa)	Peak $\phi^\circ$	Residual $c'$ (MPa)	Residual $\phi^\circ$
Basalt	Clayey basaltic breccia, wide variation from clay to basalt content	0.24	42		
Bentonite	Bentonite seam in chalk	0.015	7.5		
	Thin layers	0.09-0.12	12-17		
	Triaxial tests	0.06-0.1	9-13		
Bentonitic shale	Triaxial tests	0-0.27	8.5-29		
	Direct shear tests			0.03	8.5
Clays	Over-consolidated, slips, joints and minor shears	0-0.18	12-18.5	0-0.003	10.5-16
Clay shale	Triaxial tests	0.06	32		
	Stratification surfaces			0	19-25
Coal measure rocks	Clay mylonite seams, 10 to 25 mm	0.012	16	0	11-11.5
Dolomite	Altered shale bed, $\pm 150$ mm thick	0.04	1(5)	0.02	17
Diorite, granodiorite and porphyry	Clay gouge (2% clay, PI = 17%)	0	26.5		
Granite	Clay filled faults	0-0.1	24-45		
	Sandy loam fault filling	0.05	40		
	Tectonic shear zone, schistose and broken granites, disintegrated rock and gouge	0.24	42		
Greywacke	1-2 mm clay in bedding planes			0	21
Limestone	6 mm clay layer			0	13
	10-20 mm clay fillings	0.1	13-14		
	<1 mm clay filling	0.05-0.2	17-21		
Limestone, marl and lignite	Interbedded lignite layers	0.08	38		
	Lignite/marl contact	0.1	10		
Limestone	Marlaceous joints, 20 mm thick	0	25	0	15-24
Lignite	Layer between lignite and clay	0.014-0.03	15-17.5		
Montmorillonite Bentonite clay	80 mm seams of bentonite (montmorillonite) clay in chalk	0.36 0.016-0.02	14 7.5-11.5	0.08	11
Schists, quartzites and siliceous schists	100-15- mm thick clay filling	0.03-0.08	32		
	Stratification with thin clay	0.61-0.74	41		
	Stratification with thick clay	0.38	31		
Slates	Finely laminated and altered	0.05	33		
Quartz / kaolin / pyrolusite	Remoulded triaxial tests	0.042-0.09	36-38		

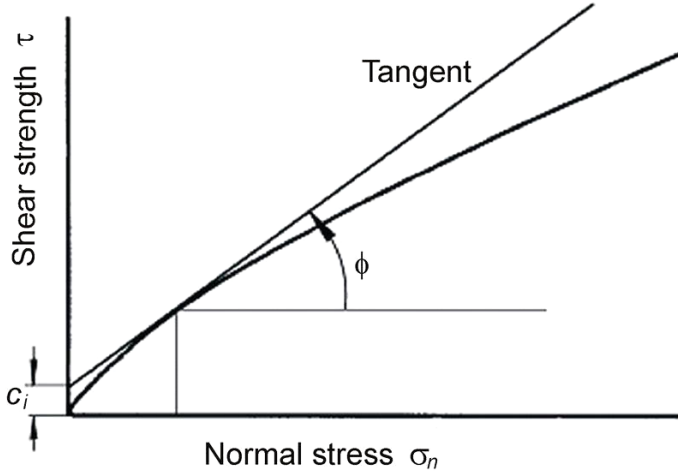


Figure 8: Definition of instantaneous cohesion  $c_i$  and instantaneous friction angle  $\phi_i$  for a non-linear failure criterion.

Note that equation 6 is not valid for  $\sigma_n = 0$  and it ceases to have any practical meaning for  $\phi_r + JRC \log_{10}(JCS/\sigma_n) > 70^\circ$ . This limit can be used to determine a minimum value for  $\sigma_n$ . An upper limit for  $\sigma_n$  is given by  $\sigma_n = JCS$ .

In a typical practical application, a spreadsheet program can be used to solve Equation 6 and to calculate the instantaneous cohesion and friction values for a range of normal stress values. A portion of such a spreadsheet is illustrated in Figure 9. In this spreadsheet the instantaneous friction angle  $\phi_i$ , for a normal stress of  $\sigma_n$ , has been calculated from the relationship:

$$\phi_i = \arctan\left(\frac{\partial \tau}{\partial \sigma_n}\right) \quad (10)$$

$$\frac{\partial \tau}{\partial \sigma_n} = \tan\left(JRC \log_{10} \frac{JCS}{\sigma_n} + \phi_r\right) - \frac{\pi JRC}{180 \ln 10} \left[ \tan^2\left(JRC \log_{10} \frac{JCS}{\sigma_n} + \phi_r\right) + 1 \right] \quad (11)$$

The instantaneous cohesion  $c_i$  is calculated from:

$$c_i = \tau - \sigma_n \tan \phi_i \quad (12)$$

In choosing the values of  $c_i$  and  $\phi_i$  for use in a particular application, the average normal stress  $\sigma_n$  acting on the discontinuity planes should be estimated and used to determine the appropriate row in the spreadsheet. For many practical problems in the field, a single average value of  $\sigma_n$  will suffice but, where critical stability problems are being considered, this selection should be made for each important discontinuity surface.

### Barton shear failure criterion

#### Input parameters:

Residual friction angle (PHIR) - degrees	29
Joint roughness coefficient (JRC)	16.9
Joint compressive strength (JCS)	96
Minimum normal stress (SIGNMIN)	0.360

Normal stress (SIGN) MPa	Shear strength (TAU) MPa	$\frac{dTAU}{dSIGN}$ (DTDS)	Friction angle (PHI) degrees	Cohesive strength (COH) MPa
0.360	0.989	1.652	58.82	0.394
0.720	1.538	1.423	54.91	0.513
1.440	2.476	1.213	50.49	0.730
2.880	4.073	1.030	45.85	1.107
5.759	6.779	0.872	41.07	1.760
11.518	11.344	0.733	36.22	2.907
23.036	18.973	0.609	31.33	4.953
46.073	31.533	0.496	26.40	8.666

#### Cell formulae:

$$SIGNMIN = 10^{(LOG(JCS) - ((70 - PHIR) / JRC))}$$

$$TAU = SIGN * TAN((PHIR + JRC * LOG(JCS / SIGN)) * PI() / 180)$$

$$DTDS = \frac{TAN((JRC * LOG(JCS / SIGN) + PHIR) * PI() / 180) - (JRC / LN(10)) * (TAN((JRC * LOG(JCS / SIGN) + PHIR) * PI() / 180)^2 + 1) * PI() / 180}{SIGN}$$

$$PHI = ATAN(DTDS) * 180 / PI()$$

$$COH = TAU - SIGN * DTDS$$

Figure 9: Printout of spreadsheet cells and formulae used to calculate shear strength, instantaneous friction angle and instantaneous cohesion for a range of normal stresses.

## References

- Barton, N. 1976. The shear strength of rock and rock joints. *Int. J. Rock Mech. Min. Sci. & Geomech. Abstr.* **13**, 1-24.
- Barton, N.R. 1973. Review of a new shear strength criterion for rock joints. *Eng. Geol.* **7**, 287-332.
- Barton, N.R. 1974. A review of the shear strength of filled discontinuities in rock. *Norwegian Geotech. Inst. Publ. No. 105*. Oslo: Norwegian Geotech. Inst.
- Barton, N.R. 1976. The shear strength of rock and rock joints. *Int. J. Mech. Min. Sci. & Geomech. Abstr.* **13**(10), 1-24.
- Barton, N.R. and Bandis, S.C. 1982. Effects of block size on the shear behaviour of jointed rock. *23rd U.S. symp. on rock mechanics*, Berkeley, 739-760.
- Barton, N.R. and Bandis, S.C. 1990. Review of predictive capabilities of JRC-JCS model in engineering practice. In *Rock joints, proc. int. symp. on rock joints*, Loen, Norway, (eds N. Barton and O. Stephansson), 603-610. Rotterdam: Balkema.
- Barton, N.R. and Choubey, V. 1977. The shear strength of rock joints in theory and practice. *Rock Mech.* **10**(1-2), 1-54.
- Deere, D.U. and Miller, R.P. 1966. Engineering classification and index properties of rock. *Technical Report No. AFNL-TR-65-116*. Albuquerque, NM: Air Force Weapons Laboratory.
- Hencher, S.R. & Richards, L.R. 1982. The basic frictional resistance of sheeting joints in Hong Kong granite *Hong Kong Engineer*, Feb., pp 21-25.
- International Society for Rock Mechanics Commission on Standardisation of Laboratory and Field Tests. 1978. Suggested methods for the quantitative description of discontinuities in rock masses. *Int. J. Rock Mech. Min. Sci. & Geomech. Abstr.* **15**, 319-368.
- Patton, F.D. 1966. Multiple modes of shear failure in rock. *Proc. 1st Congr. Int. Soc. Rock Mech.*, Lisbon 1, 509-513.